Saccade Reaction Times Are Influenced by Caudate Microstimulation Following and Prior to Visual Stimulus Appearance

Masayuki Watanabe and Douglas P. Munoz

Abstract

■ Several cognitive models suggest that saccade RTs are controlled flexibly not only by mechanisms that accumulate sensory evidence after the appearance of a sensory stimulus (poststimulus mechanisms) but also by mechanisms that preset the saccade control system before the sensory event (prestimulus mechanisms). Consistent with model predictions, neurons in structures tightly related to saccade initiation, such as the superior colliculus and FEF, have poststimulus and prestimulus activities correlated with RTs. It has been hypothesized that the BG influence the saccade initiation process by controlling both poststimulus and prestimulus activities of superior colliculus and FEF neurons. To examine this hypothesis directly, we delivered electrical microstimulation to the caudate nucleus, the input stage of the oculomotor BG, while monkeys performed a prosaccade (look toward a visual stimulus) and antisaccade (look away from the stimulus) paradigm. Microstimulation applied after stimulus appearance (poststimulus microstimulation) prolonged RTs regardless of saccade directions (contra/ipsi) or task instructions (pro/anti). In contrast, microstimulation applied before stimulus appearance (prestimulus microstimulation) shortened RTs, although the effects were limited to several task conditions. The analysis of RT distributions using the linear approach to threshold with ergodic rate model revealed that poststimulus microstimulation prolonged RTs by reducing the rate of rise to the threshold for saccade initiation, whereas fitting results for prestimulus microstimulation were inconsistent across different task conditions. We conclude that both poststimulus and prestimulus activities of caudate neurons are sufficient to control saccade RTs. ■

INTRODUCTION

Saccade RTs vary considerably and are usually longer than the shortest latency that is physiologically possible (Carpenter, 1981). It has been suggested that this procrastination reflects cognitive mechanisms that allow us to act flexibly rather than reflexively in response to a sensory event (Munoz & Everling, 2004; Everling & Fischer, 1998; Fischer & Weber, 1993). Several cognitive models have been suggested to infer the mechanisms underlying saccade initiation (Boucher, Palmeri, Logan, & Schall, 2007; Nakahara, Nakamura, & Hikosaka, 2006; Smith & Ratcliff, 2004; Reddi, Asrress, & Carpenter, 2003; Trappenberg, Dorris, Munoz, & Klein, 2001; Carpenter & Williams, 1995). According to these models, saccade RTs are controlled not only by mechanisms that accumulate sensory evidence (poststimulus mechanism) but also by mechanisms that preset the saccade control system before the appearance of the sensory event (prestimulus mechanism).

In line with the model predictions, neurophysiological experiments in behaving monkeys have revealed that, in structures that take part in the saccade control system, such as the superior colliculus (SC) and FEF, neural activity before and after sensory stimulus appearance (poststimulus and prestimulus activities, respectively) is correlated with RTs (Pare & Hanes, 2003; Everling & Munoz, 2000; Dorris, Pare, & Munoz, 1997; Hanes & Schall, 1996). This suggests that neural mechanisms controlling the poststimulus and the prestimulus activities of SC and FEF neurons are essential to achieve flexible control of saccades. The BG are key structures that modulate the poststimulus and the prestimulus activities of neurons in the SC and FEF (Hikosaka, Takikawa, & Kawagoe, 2000). Indeed, BG neurons show activity before and after visual stimulus appearance that determines required saccade directions (Watanabe & Munoz, 2009, 2010b; Ford & Everling, 2009; Yoshida & Tanaka, 2009; Basso & Wurtz, 2002; Sato & Hikosaka, 2002; Takikawa, Kawagoe, & Hikosaka, 2002; Handel & Glimcher, 1999; Kawagoe, Takikawa, & Hikosaka, 1998; Hikosaka, Sakamoto, & Usui, 1989a, 1989b; Hikosaka & Wurtz, 1983a). Furthermore, the activity of BG neurons before and after visual stimulus appearance is correlated with saccade RTs on a trial-by-trial basis (Watanabe & Munoz, 2009, 2010b; Itoh et al., 2003; Watanabe, Lauwereyns, & Hikosaka, 2003).

We have reported previously that electrical microstimulation delivered to the caudate nucleus influences saccade initiation (Watanabe & Munoz, 2010a). Although our previous microstimulation experiments establish the direct involvement of the caudate nucleus in the saccade initiation process, it is still unclear how the poststimulus versus

Queen's University, Kingston, Ontario, Canada

prestimulus activity of caudate neurons contributes to saccade initiation because, in our previous study, microstimulation influenced both poststimulus and prestimulus activities of caudate neurons. In this study, we clarified the impact of the poststimulus versus prestimulus activity of caudate neurons on the saccade initiation process by controlling the timings of microstimulation more precisely. We show that both poststimulus and prestimulus microstimulations influenced saccade initiation, but in different ways.

METHODS

General

All experimental procedures were conducted in accordance with the Canadian Council on Animal Care policy on the use and care of laboratory animals and approved by the Queen's University Animal Care Committee. Surgical and electrophysiological procedures were described previously (Marino, Rodgers, Levy, & Munoz, 2008). Briefly, two male monkeys (*Macaca mulatta*), weighing 13.5 and 10 kg, were implanted with scleral search coils, a head-restraining device, and a recording chamber under the gaseous isofluorene (2–2.5%) anesthesia with the analgesic buprenorphine (0.01–0.02 mg/kg im). Horizontal and vertical eye positions were sampled at 1 kHz using the search coil technique (Judge, Richmond, & Chu, 1980; Fuchs & Robinson, 1966; Robinson, 1963). The initiation and end of saccades were identified by radial eye velocity criteria (threshold: 30 deg/sec). Trials with RTs shorter than 70 msec or longer than 600 msec were excluded from the following data analyses (1.1%). The recording chamber (circular, 19 mm ID, tilted by 34° laterally and 13° anteriorly in Monkey O and 36° laterally in Monkey E) was placed on the left hemisphere in both monkeys to cover the head and body of the caudate nucleus. Using the grid system (Crist, Yamasaki, Komatsu, & Wurtz, 1988), we mapped the caudate nucleus as widely as possible in the area allowed by each chamber. We confirmed that stimulation sites were confined within the caudate nucleus by magnetic resonance imaging (MRI, 3 T, Siemens) in one monkey (Monkey O) whose implant was compatible with MRI.

Behavioral Paradigm

We trained the monkeys to perform a randomly interleaved prosaccade (look toward a stimulus) and antisaccade (look away from the stimulus) paradigm (Figure 1A; Bell, Everling, & Munoz, 2000). Each trial was preceded by a 600-msec intertrial interval during which the screen was illuminated with a diffuse light. After the removal of the background light, a fixation point appeared, and the monkeys were required to direct eyes toward the fixation point within 30 sec. After they maintained fixation for 900–1200 msec, a red stimulus was presented either 15° left or right from the fixation point, and the monkeys generated a saccade either toward the stimulus (prosaccade) or to the opposite direction of the stimulus (antisaccade) within 600 msec on the basis of the fixation point color (red: pro; green: anti). The task instruction (pro/anti) was given from fixation point appearance. After the saccade initiation, another 150- to 350-msec fixation was required on the peripheral red stimulus on prosaccade trials or on a peripheral green stimulus that appeared at the mirror position of the peripheral red stimulus only after saccade initiation on antisaccade trials. The red and the green peripheral stimuli remained visible until the end of the trial. The monkeys received a liquid reward after each correct performance.

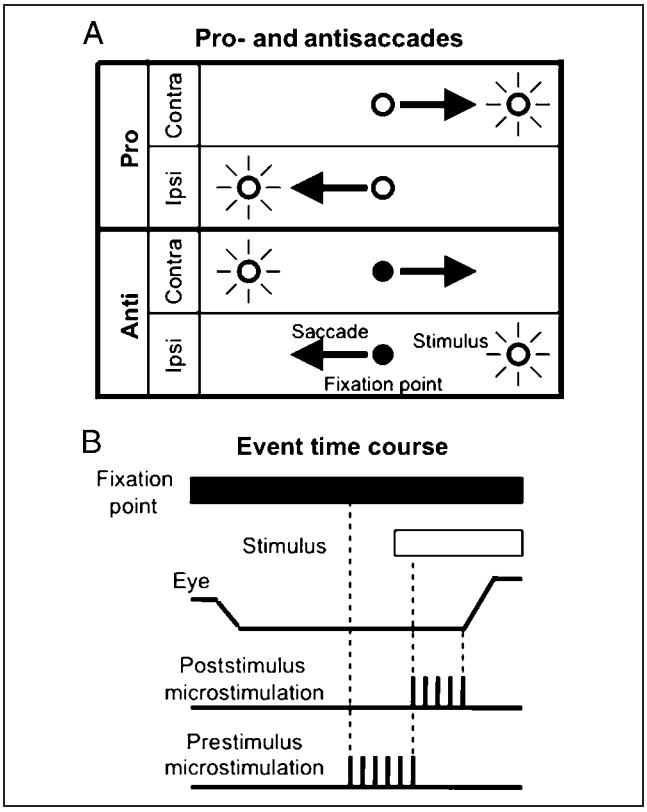

Figure 1. Prosaccade and antisaccade paradigm. (A) Four task conditions. Fixation point color indicates monkeys to perform a prosaccade (look toward a stimulus) or an antisaccade (look away from the stimulus). "Contra" and "Ipsi" indicate *saccade* directions. (B) Event time course. After fixation point appearance, monkeys acquire the fixation point and generate a saccade in response to stimulus appearance. On randomly chosen 33% of trials, microstimulation was delivered between 80 msec after stimulus appearance and saccade initiation (poststimulus microstimulation). On another 33% of trials, microstimulation was delivered between −200 and 80 msec from stimulus appearance (prestimulus microstimulation). We took into account the shortest visual latency of caudate neurons (80 msec) for the durations of poststimulus and prestimulus microstimulation.

On two thirds of the trials in a block, microstimulation was delivered either from 80 msec after stimulus appearance until saccade initiation (poststimulus stimulation) or from 200 msec before stimulus appearance until 80 msec after stimulus appearance (prestimulus stimulation; Figure 1B). We took into account the 80-msec visual delay for caudate

neurons (Watanabe & Munoz, 2009, 2010b). The pro/anti instructions, the left/right stimulus locations, and the poststimulus microstimulation/prestimulus microstimulation/control trials were randomly interleaved in the block of trials.

Electrical Microstimulation

Constant-current charge-balanced biphasic pulses (anode first, 500-μs pulse width, 50 μA, 100 Hz) were delivered to the caudate nucleus via a monopolar tungsten electrode (impedance = 0.1–1 MΩ; Frederick Haer, Bowdoin, ME) using a stimulator (Grass S88; Grass Tech., West Warwick, RI) attached to a pair of constant current stimulus isolation units (Grass PSIU6). Current was measured by the voltage drop across a 1-kΩ resistor in series with the return lead of the stimulator. The current amplitudes were lowered when the effects of microstimulation were too strong to collect enough correct trials for the analyses of RTs (10 sites among 66 sites in Monkey O). We confirmed similar results when we excluded these stimulation sites from data analyses. We adopted the stimulation parameters on the basis of previous reports (Watanabe & Munoz, 2010a; Nakamura & Hikosaka, 2006; Kitama, Ohno, Tanaka, Tsubokawa, & Yoshida, 1991). We have shown previously that caudate microstimulation with different stimulation frequencies ranging from 50 to 333 Hz produces similar effects on saccade RTs (Watanabe & Munoz, 2010a). For each penetration, we identified the caudate nucleus electrophysiologically (Watanabe & Munoz, 2009, 2010a, 2010b) and determined stimulation sites evenly along the penetration. The average distance between consecutive stimulation sites was 770 μm (SD = 530).

In quantitative analyses described later, we focused on the RTs of correct responses only because we did not find effects of microstimulation on task performance (i.e., correct performance rates). We defined correct performance rates as the number of correct trials divided by the sum of the numbers of correct, direction error, and no saccade trials. On direction error trials, monkeys made saccades toward the opposite direction of the required direction. On no saccade trials, monkeys did not generate saccades in 600 msec from stimulus appearance. Correct performance rates were not influenced by poststimulus or prestimulus microstimulation in any conditions (paired t test, $p > .05$), except for contralateral antisaccade trials in Monkey O on which prestimulus microstimulation worsened correct performance rates, $t(33) = 2.7$, $p < .05$.

RT Index

To quantify the effect of microstimulation on saccade RTs, we calculated the following index (DeAngelis & Uka, 2003):

$$\text{RT index} = \frac{M - C}{|M - C| + 2\text{RMS}_{\text{error}}} \quad (1)$$

$$\text{RMS}_{\text{error}} = \sqrt{\text{SSE}/(N - 2)} \quad (2)$$

where M and C represent average RTs on microstimulation and control trials, respectively. $\text{RMS}_{\text{error}}$ was calculated using the Equation 2. SSE is the squared sum error around the averages on control and microstimulation trials. N indicates the total number of trials. The absolute value of this index is close to 1 if the difference between the average RTs on microstimulation and control trials ($M - C$) is much larger than the variance in RTs ($\text{RMS}_{\text{error}}$), whereas it is close to zero when the difference between the average RTs is negligible compared with the variance in RTs. Positive and negative indices indicate that microstimulation prolonged and shortened RTs, respectively.

The Linear Approach to Threshold with Ergodic Rate Model

To infer the effects of microstimulation on the saccadic initiation process, we fit the linear approach to threshold with ergodic rate (LATER) model (Carpenter & Williams, 1995) to RT distributions on correct trials. The probability density function of the LATER model is given by the following equation (Nakahara et al., 2006):

$$P(t) = \frac{1}{t^2}\frac{1}{\sqrt{2\pi}\sigma_0}\exp\left\{-\frac{1}{2\sigma_0^2}\left(\frac{1}{t} - \mu_0\right)\right\} \quad (3)$$

$$\mu_0 = \frac{\mu_r}{s},\ \sigma_0 = \frac{\sigma_r}{s} \quad (4)$$

where μ_r and σ_r^2 denote the mean and the variance of the rate of rise to the threshold of saccade initiation, which obeys a Gaussian distribution, respectively, and s denotes the distance from the baseline to the threshold.

In parallel with the main LATER unit given by Equation 3, we adopted a secondary LATER unit, whose mean of the rate of rise to the threshold (μ_r) was fixed to zero, to explain short RT distributions (Carpenter & Williams, 1995). The probability density function of the two parallel LATER units is given by the following equation:

$$P(t) = P_{\text{m}}(t)1 - F_{\text{s}}(t) + P_{\text{s}}(t)1 - F_{\text{m}}(t) \quad (5)$$

where subscripts m and s denote the main and secondary LATER units, respectively, and $F(t)$ denotes a cumulative distribution function.

We fit the models to the RT distributions of correct responses on control and microstimulation trials at the same time using the following two constraints: alteration in the rate of rise (μ_r) or distance (s) of the main LATER unit (Reddi et al., 2003; Carpenter & Williams, 1995). Under the constraint of alteration in the rate of rise, μ_0 was allowed to change independently, whereas σ_0 was fixed to the same value on control and microstimulation trials. On the other hand, under

the constraint of alteration in the distance, ether μ_0 or σ_0 was allowed to change independently while the ratio of these parameters ($\mu_0/\sigma_0 = \mu_r/\sigma_r$), which does not depend on the distance *s*, was fixed to the same value on control and microstimulation trials. The σ_0 in the secondary LATER unit was allowed to change independently on control and microstimulation trials. The same conclusion was obtained when σ_0 in the secondary LATER unit was fixed to the same value on control and microstimulation trials.

We searched for a set of parameters by a simplex algorithm to maximize the logarithm of maximum likelihood estimates calculated using Equation 5. We applied this optimization procedure to the same RT distributions repeatedly with a number of different starting points to ensure the global maximum likelihood solution. We judged which constraint (alteration in the rate of rise or distance) fit to RT distributions better by subtracting the maximum log likelihood estimates of each constraint (ΔLL; Reddi et al., 2003). Positive and negative values of ΔLL support alterations in the rate of rise and distance, respectively. Using ΔLL, we also calculated the posterior probabilities of a Bayesian information criterion (BIC) by the following equation (Wagenmakers, 2007):

$$p = \frac{1}{1 + \exp\left(-\frac{1}{2}\Delta LL\right)} \quad (6)$$

If the probability is close to one, it supports the alteration in the rate of rise to the threshold for saccade initiation. On the other hand, if the probability is close to zero, it supports the alternative hypothesis of alteration in the distance between the baseline and the threshold. We also calculated Pearson's χ^2 values with parameters optimized by the procedure described earlier. We set the quantiles of 0.1, 0.3, 0.5, 0.7, and 0.9 for the calculation of χ^2 values (Ratcliff & Tuerlinckx, 2002).

RESULTS

We delivered microstimulation at 90 sites (24 and 66 in Monkey E and Monkey O, respectively) when monkeys performed the randomly interleaved pro- and antisaccade paradigm (Figure 1A). Of these, we identified 52 stimulation sites (18 and 34 in Monkey E and Monkey O, respectively), where microstimulation with either the poststimulus or the prestimulus protocol influenced saccade RTs in at least one of the four task conditions (one-way ANOVA $p < .05$ with Bonferroni correction). We focused on these 52 stimulation sites for the following quantitative analyses.

During experiments performed at the 52 stimulation sites that were analyzed, the behavior of our monkeys on control trials was consistent with previous reports in both humans (Dafoe, Armstrong, & Munoz, 2007; Fischer & Weber, 1992; Hallett, 1978) and monkeys (Bell et al., 2000). Antisaccade RTs were longer than prosaccade RTs (mean RTs ± *SD*; Monkey E: pro = 273 ± 57 msec, anti = 311 ± 80 msec, *t* test, $t(2523) = -13.8, p < .0001$; Monkey O: pro = 259 ± 68 msec, anti = 280 ± 71 msec, *t* test, $t(4436) = -9.9$, $p < .0001$). Correct performance rates (the number of correct trials divided by the sum of the numbers of correct, direction error, and no saccade trials) were worse on antisaccade trials compared with prosaccade trials (Monkey E: pro = 97%, anti = 93%, χ^2 test, $df = 2$, $\chi^2(2) = 28$, $p < .0001$; Monkey O: pro = 96%, anti = 89%, $\chi^2(2) = 98$, $p < .0001$).

Poststimulus Microstimulation

Figure 2 shows an example of a stimulation site in Monkey E where microstimulation influenced saccade RTs. At this stimulation site, poststimulus microstimulation prolonged RTs in all task conditions (*t* tests): pro–contra, $t(44) = 6.2$, $p < .0001$; pro–ipsi, $t(69) = 2.5$, $p < .05$; anti–contra, $t(49) = 5.3, p < .0001$; anti–ipsi, $t(68) = 7.4, p < .0001$.

The suppression effects of poststimulus microstimulation were observed commonly across different stimulation sites (Figure 3). We found that the distributions of RT indices were biased toward positive values in all task conditions in both monkeys, indicating that poststimulus microstimulation prolonged saccade RTs at the population level in all task conditions (*t* tests; Monkey E: pro–contra, $t(17) = 7.0, p < .0001$; pro–ipsi, $t(17) = 4.7, p < .0005$; anti–contra, $t(17) = 3.5, p < .005$; anti–ipsi, $t(17) = 7.1, p < .0001$; Monkey O: pro–contra, $t(33) = 8.8, p < .0001$; pro–ipsi, $t(33) = 2.6, p < .05$; anti–contra, $t(33) = 7.5, p < .0001$; anti–ipsi, $t(33) = 4.1, p < .0005$).

We have shown previously that the suppression effects of microstimulation on contralateral saccades are stronger on prosaccade trials compared with antisaccade trials (Watanabe & Munoz, 2010a). We confirmed these asymmetric suppression effects on saccades toward the contralateral direction in both monkeys at the population level (*t* tests; Monkey E: $t(17) = 2.5, p < .05$; Monkey O: $t(33) = 3.3, p < .005$). We did not find a significant difference in RT indices between prosaccade and antisaccade trials when saccades were directed toward the ipsilateral direction (*t* tests; Monkey E: $t(17) = -1.1, p > .2$; Monkey O: $t(33) = -1.1$, $p > .2$).

The effects of poststimulus microstimulation on the RTs of both contralateral and ipsilateral saccades do not necessarily mean that caudate neurons activated by poststimulus microstimulation at individual stimulation sites issued spatially nonspecific suppression signals. Specifically, we did not find correlation between RT indices for contralateral and ipsilateral saccades on either prosaccade or antisaccade trials, except for antisaccade trials in Monkey E (Pearson's correlation coefficient; Monkey E: pro, $n = 18, r = 0.13, p > .6$; anti, $n = 18, r = 0.69, p < .005$; Monkey O: pro, $n = 34, r = -0.18, p > .3$; anti, $n = 34, r = 0.05, p > .7$). We suggest instead that contralateral and ipsilateral saccade suppressions were mediated by mechanisms recruited independently.

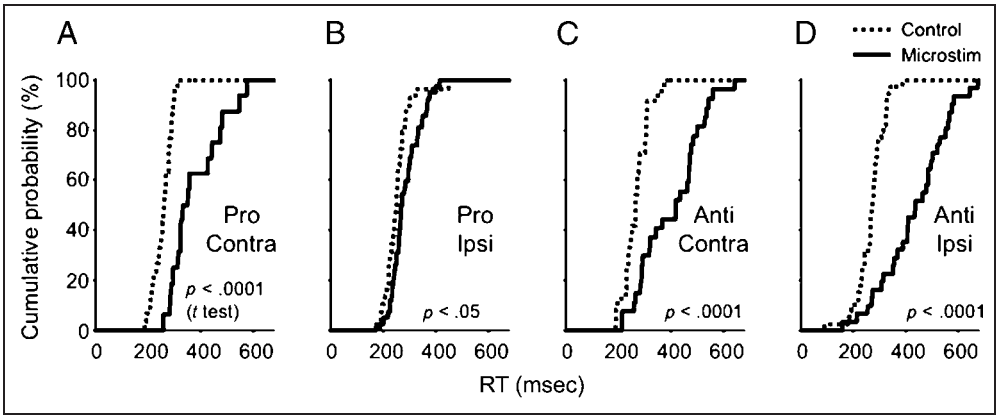

Figure 2. Examples of the effects of poststimulus microstimulation on saccade RTs. The results were delivered from a single stimulation site in Monkey E. (A) Contralateral prosaccade trials. (B) Ipsilateral prosaccade trials. (C) Contralateral antisaccade trials. (D) Ipsilateral antisaccade trials. The continuous and the broken lines indicate microstimulation and control trials, respectively.

If poststimulus microstimulation influenced visual stimulus processing, its effects on the RTs of saccades in response to the same stimulus (e.g., contralateral prosaccades and ipsilateral antisaccades) should be correlated with each other. However, we did not find such correlations, except for trials with the contralateral stimulus in Monkey E (Pearson's correlation coefficient; Monkey E: contra, $n = 18, r = 0.48, p < .05$; ipsi, $n = 18, r = 0.21, p > .3$; Monkey O, contra, $n = 34, r = -0.34, p > .05$; ipsi, $n = 34, r = 0.06, p > .7$). Instead, we found that the effects of poststimulus microstimulation on the RTs of prosaccade and antisaccades toward the same direction were correlated with each other, except for trials with ipsilateral saccades in Monkey E (Monkey E: contra, $n = 18, r = 0.67, p < .005$; ipsi, $n = 18, r = 0.34, p > .1$; Monkey O: contra, $n = 34, r = 0.59, p < .0005$; ipsi, $n = 34, r = 0.58, p < .0005$). We therefore suggest that poststimulus microstimulation influenced saccade initiation processes rather than visual stimulus detection processes.

Prestimulus Microstimulation

Figure 4 shows an example of the effects of prestimulus microstimulation on saccade RTs at the same stimulation site

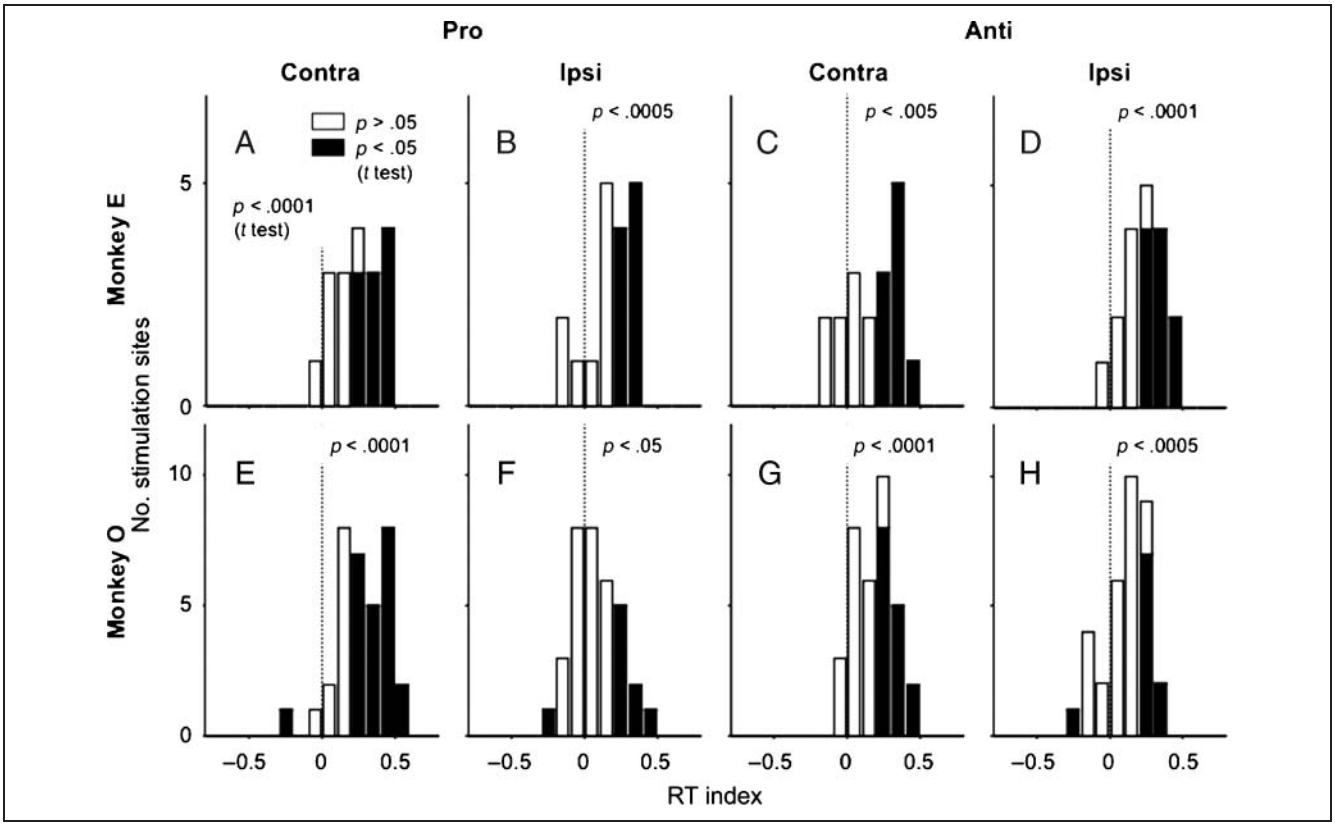

Figure 3. Summaries of the effects of poststimulus microstimulation on saccade RTs. The top and bottom rows indicate Monkey E and Monkey O, respectively. The four columns from left to right indicate contralateral prosaccade, ipsilateral prosaccade, contralateral antisaccade, and ipsilateral antisaccade trials, respectively. Black bars indicate stimulation sites with statistical significances (t test, $p < .05$).

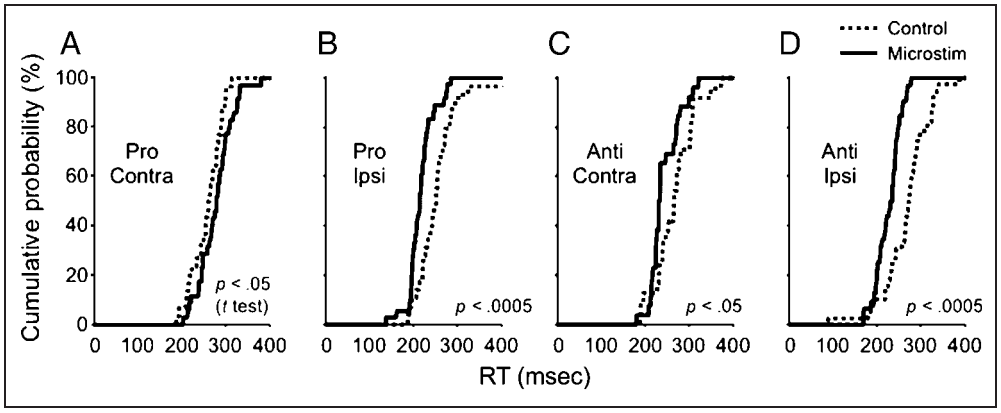

Figure 4. Examples of the effects of prestimulus microstimulation on saccade RTs. The results were delivered from the same stimulation site shown in Figure 2. (A) Contralateral prosaccade trials. (B) Ipsilateral prosaccade trials. (C) Contralateral antisaccade trials. (D) Ipsilateral antisaccade trials. The continuous and the broken lines indicate microstimulation and control trials, respectively.

shown in Figure 2. At this site, prestimulus microstimulation shortened RTs in all task conditions except for contralateral prosaccade trials on which RTs were prolonged (t tests; pro–contra, $t(63) = 2.2$, $p < .05$; pro–ipsi, $t(63) = -3.7$, $p < .0005$; anti–contra, $t(48) = -2.1$, $p < .05$; anti–ipsi, $t(69) = -4.0$, $p < .0005$).

The facilitation effects of prestimulus microstimulation were confirmed at other stimulation sites, although the effects were not consistent across stimulation sites or between monkeys (Figure 5). In Monkey E, we found that RT indices were biased toward negative values in all task conditions except for contralateral prosaccade trials (t test results; pro–contra, $t(17) = 1.1$, $p > 0.2$; pro–ipsi, $t(17) = -3.0$, $p < .01$; anti–contra, $t(17) = -6.4$, $p < .0001$; anti–ipsi, $t(17) = -8.0$, $p < .0001$). However, in Monkey O, we found that prestimulus microstimulation shortened RTs only on ipsilateral antisaccade trials (t tests; pro–contra, $t(33) = 0.5$, $p > 0.6$; pro–ipsi, $t(33) = -1.7$, $p > .05$; anti–contra, $t(33) = 1.0$, $p > .3$; anti–ipsi, $t(33) = -4.4$, $p < .0005$).

The facilitation effects were stronger on antisaccade trials compared with prosaccade trials for both saccade directions in Monkey E (paired t tests; contra, $t(17) = 3.8$, $p < .005$; ipsi, $t(17) = 3.5$, $p < .005$) but not in Monkey O

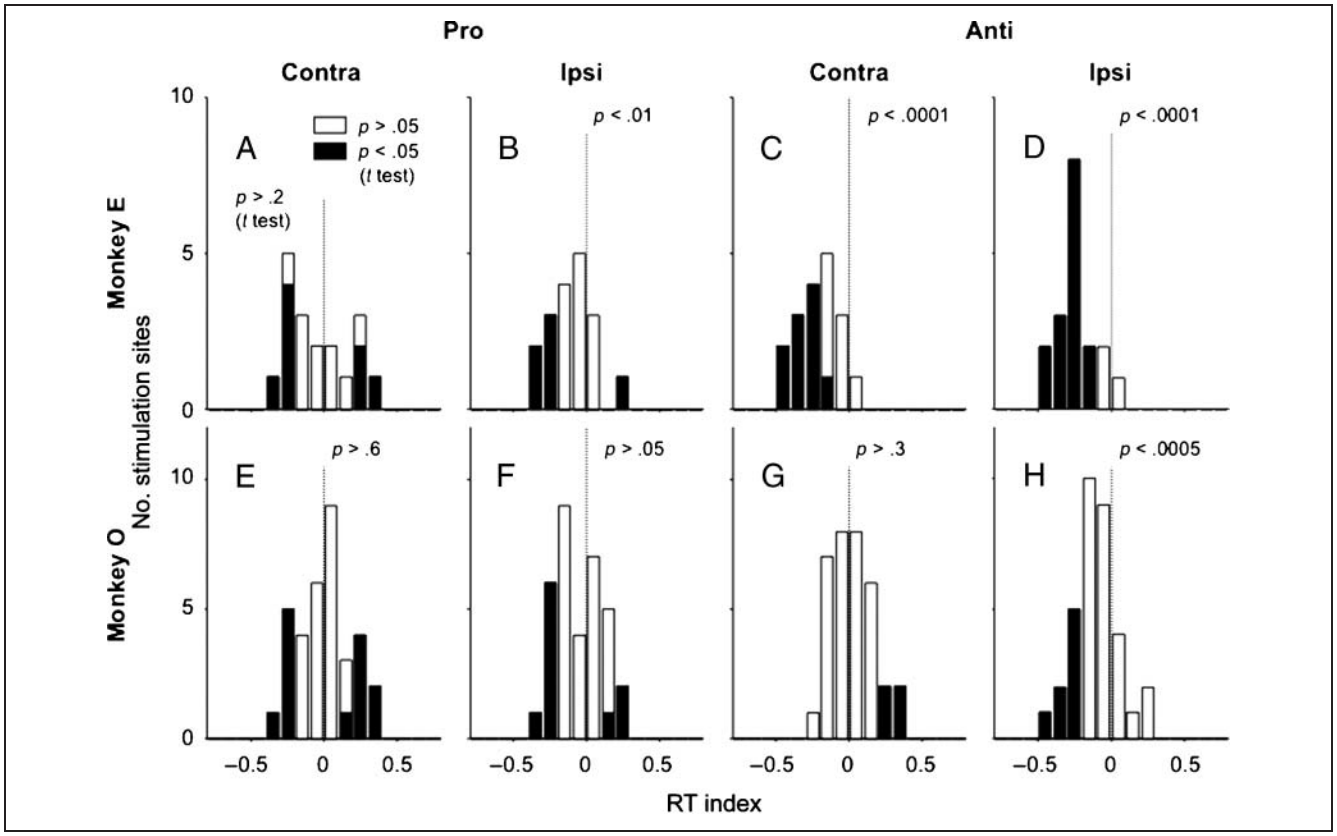

Figure 5. Summaries of the effects of prestimulus microstimulation on saccade RTs. The top and bottom rows indicate Monkey E and Monkey O, respectively. The four columns from left to right indicate contralateral prosaccade, ipsilateral prosaccade, contralateral antisaccade, and ipsilateral antisaccade trials, respectively. Black bars indicate stimulation sites with statistical significances (t test, $p < .05$).

(contra, $t(33) = -0.4$, $p > .7$; ipsi, $t(33) = 2.0$, $p > .05$). RT indices for contralateral and ipsilateral saccades were not correlated with each other on either prosaccade or antisaccade trials (Pearson's correlation coefficient; Monkey E: pro, $n = 18$, $r = -0.03$, $p > .9$; anti, $n = 18$, $r = 0.13$, $p > .6$; Monkey O: pro, $n = 34$, $r = -0.08$, $p > .6$; anti, $n = 34$, $r = 0.16$, $p > .3$).

The effects of prestimulus microstimulation on prosaccade and antisaccades in response to the same stimulus were not correlated with each other (Monkey E: contra, $n = 18$, $r = 0.19$, $p > .4$; ipsi, $n = 18$, $r = -0.24$, $p > .3$; Monkey O: contra, $n = 34$, $r = -0.04$, $p > .8$; ipsi, $n = 34$, $r = -0.11$, $p > .5$). In contrast, the effects of prestimulus microstimulation on prosaccade and antisaccades toward the same direction were correlated with each other, except for the ipsilateral direction in Monkey E (Monkey E: contra, $n = 18$, $r = 0.65$, $p < .005$; ipsi, $n = 18$, $r = 0.34$, $p > .1$; Monkey O: contra, $n = 34$, $r = 0.50$, $p < .005$; ipsi, $n = 34$, $r = 0.38$, $p < .05$). These results therefore also suggest that prestimulus microstimulation influenced saccade initiation processes rather than visual stimulus detection processes.

Although the results of prestimulus microstimulation were not as consistent as those of poststimulus microstimulation, they indicate that the activity of caudate neurons before stimulus appearance is sufficient to influence the saccade initiation process.

Comparison between Poststimulus and Prestimulus Microstimulation

We found opposite effects on saccade RTs by poststimulus and prestimulus microstimulation (compare Figures 2–5). To examine this counterintuitive observation further, we compared the effects of poststimulus and prestimulus microstimulation on saccade RTs (Figure 6). We found that RT indices for poststimulus and prestimulus microstimulation were correlated positively when saccades were directed toward the contralateral direction on both prosaccade (Figure 6A) and antisaccade (Figure 6B) trials in both monkeys (Pearson's correlation coefficient; Monkey E: pro, $n = 18$, $r = 0.54$, $p < .05$; anti, $n = 18$, $r = 0.55$, $p < .05$; Monkey O: pro, $n = 34$, $r = 0.65$, $p < .0001$; anti, $n = 34$, $r = 0.48$, $p < .005$). This indicates that the saccade suppression effects of poststimulus microstimulation were stronger when the saccade facilitation effects of prestimulus microstimulation were weaker. Such a relationship was not observed for ipsilateral saccades (Monkey E; pro, $n = 18$, $r = 0.16$, $p > .5$; anti, $n = 18$, $r = 0.06$, $p > .8$; Monkey O; pro, $n = 34$, $r = 0.20$, $p > .2$; anti, $n = 34$, $r = 0.11$, $p > .5$).

The positive correlation observed in RT indices for contralateral saccades suggests that common neural circuits suppressing contralateral saccades were recruited by poststimulus and prestimulus microstimulation, which might have masked the facilitation effects of prestimulus

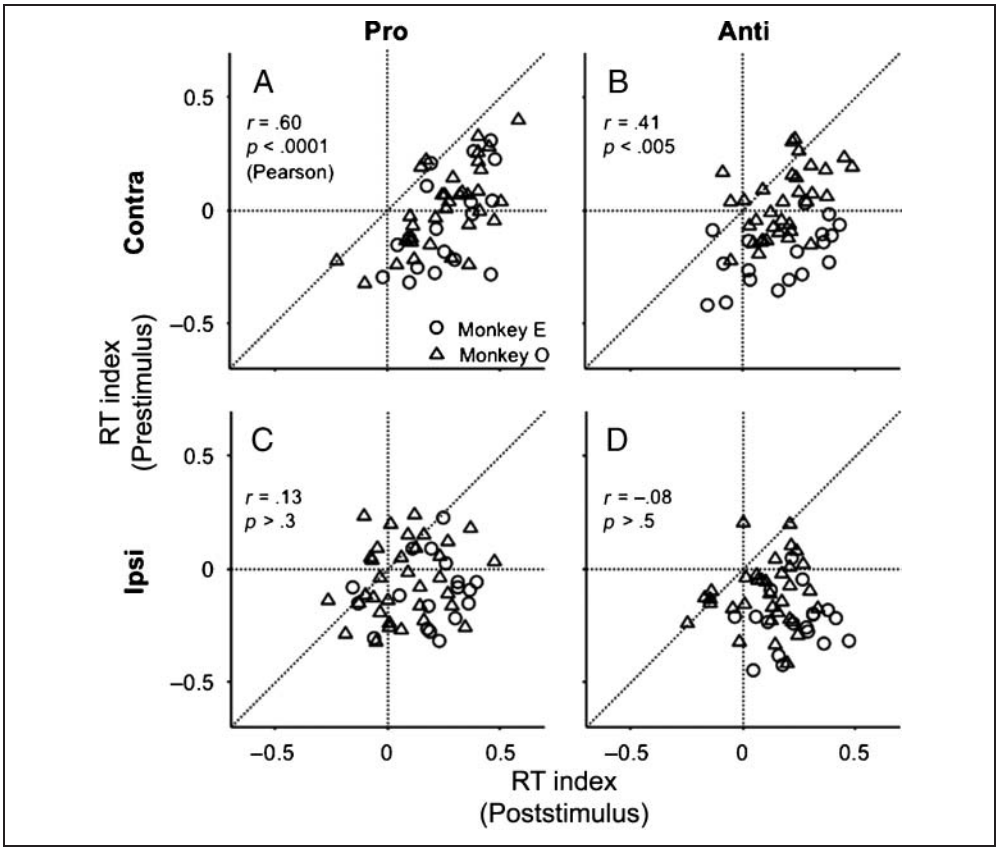

Figure 6. Comparison between the effects of poststimulus and prestimulus microstimulation on RTs. (A) Contralateral prosaccade trials. (B) Contralateral antisaccade trials. (C) Ipsilateral prosaccade trials. (D) Ipsilateral antisaccade trials. The *x*- and the *y*-axes indicate RT indices for poststimulus and prestimulus microstimulation, respectively. Circles and triangles indicate data from Monkey E and Monkey O, respectively. Pearson's correlation coefficients shown in this figure were calculated using data from two monkeys. Correlation coefficients calculated in each monkey are shown in the main text.

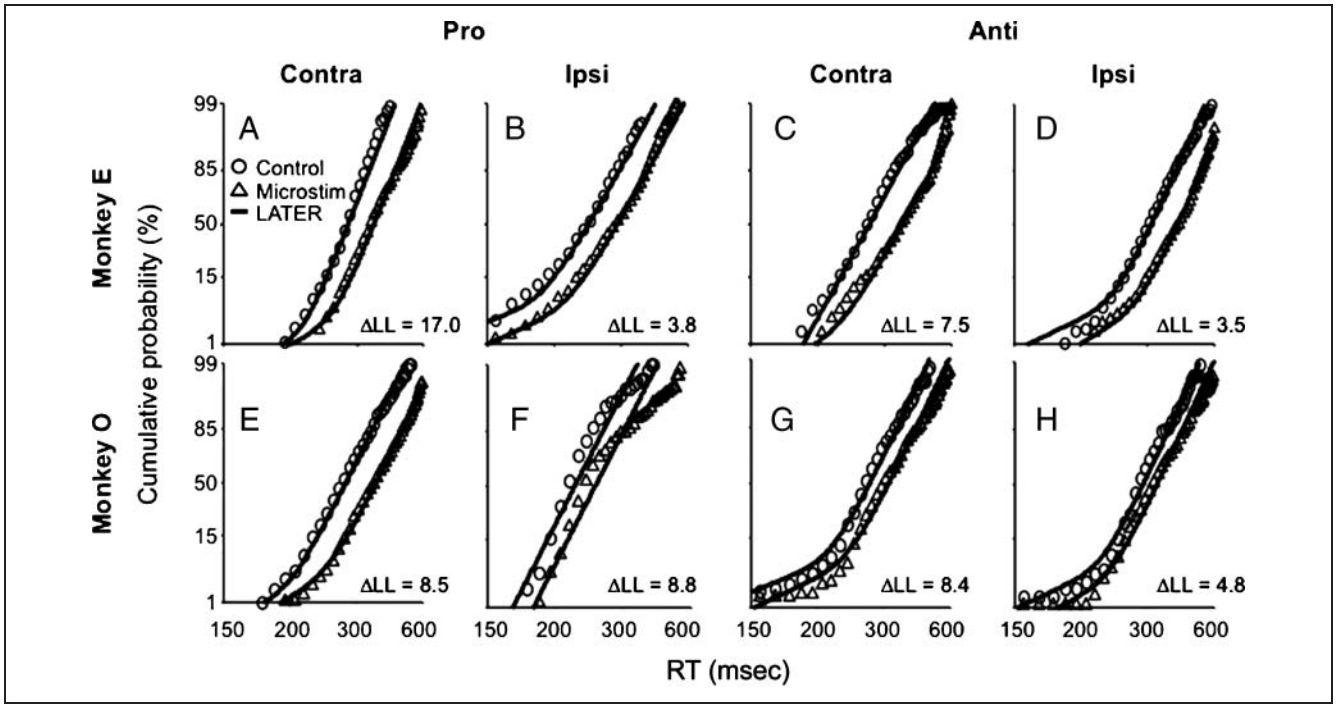

Figure 7. LATER model fittings for poststimulus microstimulation. The top and the bottom rows indicate Monkey E and Monkey O, respectively. The four columns from left to right indicate contralateral prosaccade, ipsilateral prosaccade, contralateral antisaccade, and ipsilateral antisaccade trials, respectively. For each condition, stimulation sites were included in this analysis if poststimulus microstimulation prolonged RTs (indicated by black bars with positive RT indices in Figure 3). Circles and triangles indicate cumulative distributions of RTs with 10 msec bin width on control and microstimulation trials, respectively. Continuous lines indicate the fitting results of LATER model under the constraint of alteration only in the rate of rise to the threshold for saccade initiation, which was supported by the all data sets in this figure (positive values of ΔLL).

microstimulation on contralateral prosaccade trials in Monkey E (Figure 5A) and contralateral prosaccade (Figure 5E) and antisaccade (Figure 5G) trials in Monkey O.

LATER Model

To infer how microstimulation influenced the saccadic decision process, we analyzed RT distributions using the LATER model (Nakahara et al., 2006; Reddi et al., 2003; Carpenter & Williams, 1995). The model assumes a constant baseline activity and linear rise of a decision signal. Saccades are triggered when the decision signal reaches a threshold. According to this model, RTs can be prolonged or shortened by changing the rate of rise in the decision signal or the distance between the baseline and the threshold for saccade initiation. These two mechanisms produce characteristic effects on RT distributions on the reciprobit (Figures 7 and 8; Nakahara et al., 2006; Reddi et al., 2003; Carpenter & Williams, 1995). If microstimulation changed the rate of rise to the threshold for saccade initiation, the two RT distributions for control and microstimulation trials shift along the *x*-axis. On the other hand, if microstimulation changed the distance between the baseline and the threshold for saccade initiation, the two RT distributions on control and microstimulation trials should swivel at a common *y*-intercept.

Figure 7A shows an example of a LATER model fitting to the RT distributions of contralateral prosaccades on control and poststimulus microstimulation trials in Monkey E. For this analysis, in Figure 7A, we collapsed stimulation sites where poststimulus microstimulation prolonged RTs (n = 10, indicated by black bars in Figure 3A). We found that, in this data set, poststimulus microstimulation caused parallel shift rather than swiveling on the reciprobit. This suggests that poststimulus microstimulation prolonged RTs by decreasing the rate of rise to the threshold for saccade initiation. This qualitative observation was confirmed quantitatively by the fact that the maximum log likelihood under the constraint of alteration only in the rate of rise to the threshold was higher compared with the constraint of alteration only in the distance between the baseline and the threshold (ΔLL = 17.0). Similar results were confirmed in the rest of the data sets (black bars with positive RT indices in Figure 3) in which poststimulus microstimulation prolonged saccade RTs (Figure 7; for the summary of fitting results, see Table 1). These results are consistent with our previous report in which the suppression effects of microstimulation were explained mainly by alteration in the rate of rise to the threshold (Watanabe & Munoz, 2010a).

Figure 8C shows another example of a LATER model fitting to the RT distributions of ipsilateral antisaccades on control and prestimulus microstimulation trials in Monkey E. For this analysis, in Figure 8C, we collapsed stimulation sites where prestimulus microstimulation shortened RTs (n = 15, indicated by black bars in Figure 5D). It can be seen clearly that prestimulus microstimulation caused

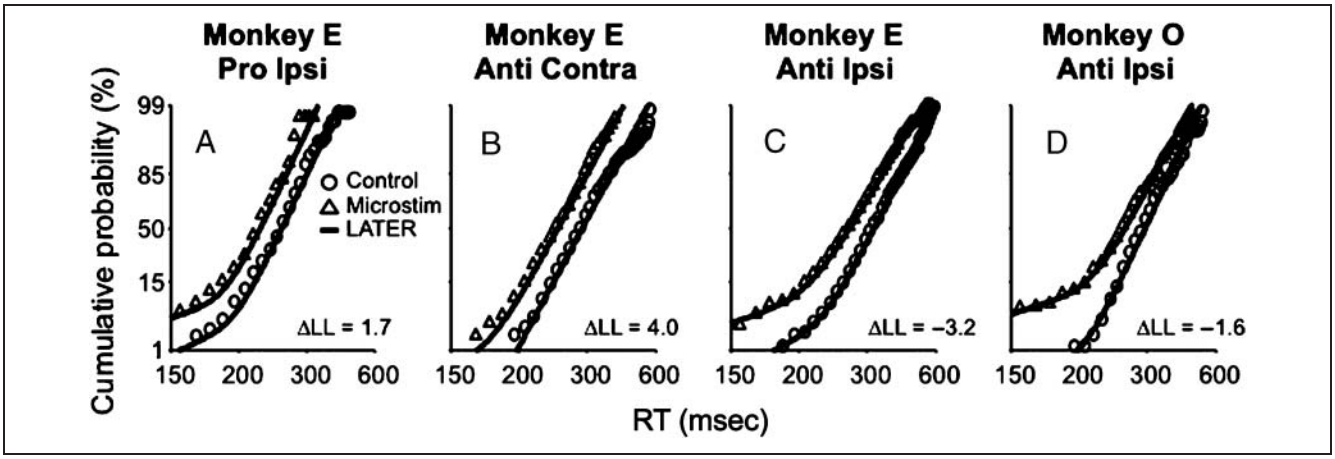

Figure 8. LATER model fittings for prestimulus microstimulation. (A) Ipsilateral prosaccade trials in Monkey E. (B) Contralateral antisaccade trails in Monkey E. (C) Ipsilateral antisaccade trials in Monkey E. (D) Ipsilateral antisaccade trials in Monkey O. These conditions were chosen for this analysis because prestimulus microstimulation shortened RTs at the population level (t test, $p < .05$; Figure 5). The fitting results of the LATER model support alteration in the rate of rise to the threshold for saccade initiation in panels A and B (positive values of ΔLL) and alteration in the distance between the baseline and the threshold in panels C and D (negative values of ΔLL).

swiveling rather than parallel shift on the reciprobit. This suggests that prestimulus microstimulation shortened RTs by decreasing the distance between the baseline and the threshold for saccade initiation in this specific task condition (ΔLL = −3.2). We carried out the same analysis for conditions in which prestimulus microstimulation shortened saccade RTs at the population level (ipsilateral prosaccade and contralateral and ipsilateral antisaccade trials in Monkey E and ipsilateral antisaccade trials in Monkey O; see Figure 5). For this analysis, we collapsed data from stimulation sites where prestimulus microstimulation shortened RTs (black bars in Figure 5). In contrast with poststimulus microstimulation, the results of LATER model fittings were not consistent across data sets for prestimulus microstimulation (Figure 8; for the summary of fitting results, see Table 1).

Stimulation Sites

We reconstructed the 52 stimulation sites where poststimulus and/or prestimulus microstimulation influenced saccade RTs in at least one of the four conditions during the prosaccade and antisaccade paradigm (Figure 9). To

Table 1. Summary of LATER Model Fittings

Stim	*Monk*	*Inst*	*Dir*	*N Sites*	*N Control*	*N Stim*	χ^2 *Rate*	χ^2 *Dist*	*ΔLL*	*BIC Prob*
Post	E	Pro	Contra	10	350	344	43.2	79.9	17	1.0
Post	E	Pro	Ipsi	9	325	372	12.8	19.0	3.8	0.98
Post	E	Anti	Contra	9	321	284	18.3	33.0	7.5	1.0
Post	E	Anti	Ipsi	10	377	334	16.7	30.6	3.5	0.97
Post	O	Pro	Contra	22	719	697	15.1	47.3	8.5	1.0
Post	O	Pro	Ipsi	8	290	114	135	238	8.8	1.0
Post	O	Anti	Contra	15	465	418	59.5	80.7	8.4	1.0
Post	O	Anti	Ipsi	9	251	279	39.3	47.3	4.8	0.99
Pre	E	Pro	Ipsi	5	143	177	5.7	5.9	1.7	0.84
Pre	E	Anti	Contra	10	324	328	7.8	9.3	4.0	0.98
Pre	E	Anti	Ipsi	15	552	498	10.2	8.4	−3.2	0.04
Pre	O	Anti	Ipsi	8	232	243	16.1	15.9	−1.6	0.16

Stim = stimulation protocols (poststimulus/prestimulus); Monk = monkeys; Inst = task instructions; Dir = saccade directions; N Sites = number of stimulation sites; N Control = number of control trials; N Stim = number of stimulation trials. χ^2 Rate = Pearson chi-square statistics for the constraints of alteration in the rate of rise to the threshold; χ^2 Dist = Pearson chi-square statistics for the constraints of alteration in the distance between the baseline and the threshold for saccade initiation.

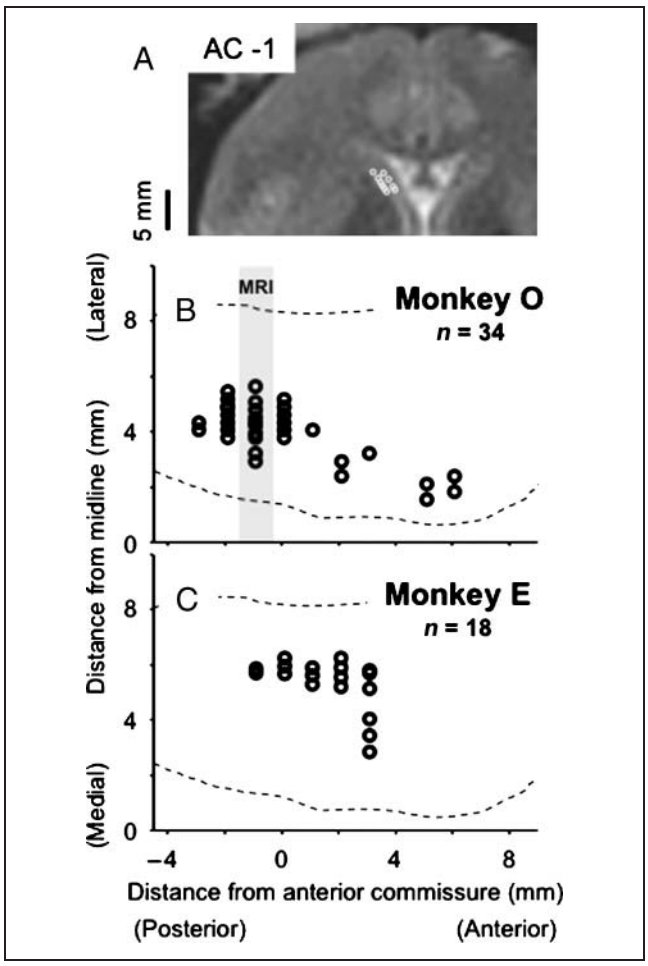

Figure 9. Reconstructed stimulation sites. (A) MRI image at 1 mm posterior from the anterior commissure in Monkey O. (B, C) Reconstructed sites projected on the horizontal plane in Monkey O (n = 34) (B) and Monkey E (n = 18) (C), respectively. Sites included in the gray stripes labeled as MRI in panel B are superimposed on the MRI image (A). Broken lines indicate the boundaries of the caudate nucleus (Francois, Yelnik, & Percheron, 1996). In Monkey E, the level of the anterior commissure is estimated at 19 mm anterior from the intermeatal line (Mikula, Trotts, Stone, & Jones, 2007).

examine whether the effects of poststimulus and prestimulus microstimulation depended on the coordinates of stimulation sites, we calculated Spearman's partial correlation coefficients between RT indices in each condition and one of the coordinates of the stimulation sites (rostral–caudal, medial–lateral, and dorsal–ventral) with the remaining coordinates of the stimulation sites fixed. We did not find significant correlation between the RT indices and the coordinates of the stimulation sites ($p > .05$), except for the following in each monkey. In Monkey E, prestimulus microstimulation facilitated ipsilateral antisaccade initiation more strongly at the posterior–lateral–ventral stimulation sites (Spearman's partial correlation coefficients for each axis, $n = 18$; rostral–caudal, $r = 0.52, p < .05$; medial–lateral, $r = -0.55$, $p < .05$; dorsal–ventral, $r = 0.56$, $p < .05$). In Monkey O, poststimulus microstimulation suppressed contralateral prosaccade and antisaccades more strongly at lateral stimulation sites (n = 34, lateral-medial; pro, $r = 0.36$, $p < .05$; anti, $r = 0.46$, $p < .01$).

DISCUSSION

We found that microstimulation delivered to the caudate nucleus before and after stimulus appearance influenced saccade RTs, but in very different ways. Poststimulus microstimulation prolonged RTs in all task conditions (Figure 3). In contrast, prestimulus microstimulation shortened RTs in limited task conditions (Figure 5). Fitting the LATER model to RT distributions revealed that poststimulus microstimulation suppressed saccade initiation by attenuating the rate of rise to the threshold for saccade initiation (Figure 7). In contrast, the results of LATER model fittings were inconsistent across different data sets for prestimulus microstimulation (Figure 8). In the following discussion, we propose several neural mechanisms that might account for our paradoxical pattern of findings.

Saccade Suppression by Poststimulus Microstimulation

The effects of poststimulus microstimulation (Figures 3 and 7) are very similar to what we found previously when microstimulation was delivered continuously during both poststimulus and prestimulus periods (Watanabe & Munoz, 2010a). This suggests that the suppression effects of microstimulation reported previously were mainly caused by microstimulation delivered after stimulus appearance.

As we hypothesized previously, there are at least two possibilities to account for the suppression effects (Watanabe & Munoz, 2010a). First, microstimulation activated caudate neurons giving rise to the direct pathway, which facilitated saccade initiation, and those giving rise to the indirect pathway, which suppressed saccade initiation, with equal intensity. However, the artificial signals carried by the indirect pathway are dominant over those carried by the direct pathway to account for the saccade suppression effects. The polysynaptic indirect pathway takes longer to influence behavior than the direct pathway (Tachibana, Kita, Chiken, Takada, & Nambu, 2008). Nevertheless, it is possible that the indirect pathway is recruited by poststimulus microstimulation to induce saccade suppression on the basis of the following reasons. The latency of caudate neurons to influence eye movements could be as little as 26 msec on the basis of previous studies (Miyashita & Hikosaka, 1996; Hikosaka, Sakamoto, & Miyashita, 1993; Hikosaka & Wurtz, 1983b). The indirect pathway presumably needs additional 15 msec to influence eye movements (Tachibana et al., 2008). Poststimulus microstimulation was initiated from 80 msec after stimulus appearance (Figure 1B). Accordingly, the direct and the indirect pathways could influence saccades with RTs longer than 106 and 121 msec, respectively, by poststimulus microstimulation. Both of these latencies are long enough to influence the majority of saccades initiated 200 msec after stimulus appearance (e.g., Figures 2 and 4).

Second, microstimulation recruited lateral inhibitory interactions within the caudate nucleus itself, which attenuated the activity of caudate neurons remote from the stimulation site. If these neurons give rise to the direct pathway, their saccade facilitation signals were attenuated by microstimulation. Both of the above mechanisms could lead to increased RTs and therefore saccade suppression.

Saccade suppression by poststimulus microstimulation was observed in both contralateral and ipsilateral saccades (Figure 3). As we suggested in the Results section, this does not necessarily mean that microstimulation recruited neurons that issue spatially nonspecific suppression signals because there was no correlation between suppression effects on contralateral and ipsilateral saccades (except for antisaccade trials in Monkey E; see Results). Instead, we suggest that microstimulation recruited neural mechanisms suppressing contralateral saccades and those suppressing ipsilateral saccades independently. It has been shown that the majority of neurons in the substantia nigra pars reticulata (SNr), the output structure of the oculomotor BG, influence the SC and FEF in the same hemisphere, whereas a subset of SNr neurons influence those structures in the opposite hemisphere (Cebrian, Parent, & Prensa, 2005; Jiang, Stein, & McHaffie, 2003). We speculate that different populations of caudate neurons giving rise to the indirect pathway control the two types of SNr neurons independently.

It seems likely that the activation of neural mechanisms suppressing saccade initiation persisted until microstimulation was turned off after saccade initiation. This enhanced tonic suppression on neurons in the SC and FEF (via thalamus) could interfere with the accumulation rate of presaccadic activity. We speculate that the analyses using the LATER model (Figure 7) detected such interference of presaccadic processing in the SC and FEF by poststimulus microstimulation.

Saccade Facilitation by Prestimulus Microstimulation

In contrast with poststimulus microstimulation, we found that prestimulus microstimulation facilitated saccade initiation on ipsilateral prosaccade, contralateral, and ipsilateral antisaccade trials in Monkey E and ipsilateral antisaccade trials in Monkey O (Figure 5). It is likely that poststimulus and prestimulus microstimulation activated the same population of caudate neurons around the tip of a microelectrode at each stimulation site. However, it is counterintuitive to explain the facilitation effects of prestimulus microstimulation by the same mechanisms we hypothesized to explain the suppression effects of poststimulus microstimulation. A possibility might be that termination of microstimulation trains immediately after stimulus appearance by prestimulus microstimulation (Figure 1B) might have released SC and FEF neurons from enhanced suppression, which in turn induced rebound activity in the same neurons, thereby facilitating saccade initiation (rebound activity after GABAergic inhibition has been reported in the thalamus; Person & Perkel, 2005). The variability of such rebound activity might also explain the inconsistent effects of prestimulus microstimulation on saccade RTs (Figures 5 and 8).

Another possibility might be that the effects of the direct pathway on saccade RTs might be predominant over the indirect pathway before stimulus appearance. Caudate neurons giving rise to the direct pathway project directly to the SNr (Hikosaka et al., 2000). In contrast, caudate neurons giving rise to the indirect pathway influence the activity of SNr neurons via the external segment of globus pallidus and subthalamic nucleus (STN; Hikosaka et al., 2000). It is reasonable to assume that the monosynaptic connections in the direct pathway carry artificial caudate signals created by prestimulus microstimulation without further modifications along the axons. However, artificial signals induced by caudate microstimulation transmitted through the indirect pathway might be controlled by endogenous signals, such as those carried by the hyperdirect pathway connecting between the cortex and the STN directly (Nambu et al., 2000). Spatial information arriving in the STN after stimulus appearance might enhance the artificial suppression signals created by caudate microstimulation, which might then switch the dominance between the direct and the indirect pathways in the SNr, leading from saccade facilitation to saccade suppression.

Comparison with Previous Reports

The effects of microstimulation on saccade RTs have been examined in a number of structures involved in saccade control (Phillips, Johnston, & Everling, 2011; Wegener, Johnston, & Everling, 2008; Yang, Heinen, & Missal, 2008; Basso & Liu, 2007; Dorris, Olivier, & Munoz, 2007; Nakamura & Hikosaka, 2006; Stuphorn & Schall, 2006; Isoda, 2005; Izawa, Suzuki, & Shinoda, 2004a, 2004b; Burman & Bruce, 1997; Munoz & Wurtz, 1993). Of these, results similar to our findings have been reported in the pre-SMA (Isoda, 2005). Microstimulation delivered to the pre-SMA before the onset of a go signal, which allows monkeys to generate a saccade toward a peripheral visual stimulus, shortens RTs, whereas the same microstimulation delivered after the go signal prolongs RTs regardless of saccade directions. Because of this similarity, it is reasonable to speculate that the effects of microstimulation observed in the pre-SMA and caudate nucleus might be mediated by the common cortex–BG loops (Nachev, Kennard, & Husain, 2008; Alexander, DeLong, & Strick, 1986). An important difference between the caudate nucleus and the pre-SMA is that microstimulation applied to the caudate nucleus evokes contralateral saccades during free viewing (Kitama et al., 1991), but such effects are not induced by microstimulation applied to the pre-SMA (Luppino, Matelli, Camarda, Gallese, & Rizzolatti, 1991). This might indicate that the effects of microstimulation applied to the pre-SMA on saccade RTs might be realized through the caudate nucleus in a task-dependent manner.

Similar bidirectional saccade suppression by microstimulation is also reported previously in the pre-SMA using a simple visually guided saccade paradigm (Yang et al., 2008) and in the supplementary eye field using a countermanding saccade paradigm (Stuphorn & Schall, 2006).

Microstimulation applied to other cortical areas, such as the FEF (Izawa et al., 2004a, 2004b; Burman & Bruce, 1997) and dorsolateral pFC (Wegener et al., 2008), causes effects on saccade RTs dissimilar to what we found in the caudate nucleus. It is possible that the effects of microstimulation applied to these cortical areas are realized by their direct projections to the SC bypassing the BG (Johnston & Everling, 2006; Everling & Munoz, 2000; Huerta & Kaas, 1990). However, the dissimilarity of microstimulation effects between the caudate nucleus and the cortical areas does not exclude a possibility that the caudate nucleus mediates at least some of the effects of the cortical microstimulation. For instance, suppression of ipsilateral saccades has been observed commonly in these structures (Wegener et al., 2008; Izawa et al., 2004a, 2004b; Burman & Bruce, 1997). This ipsilateral saccade suppression might be realized by selective activation of caudate neurons that give rise to the indirect pathway controlling the SC and/or FEF in the opposite hemisphere. Such selective activation of caudate neurons would not be achieved by microstimulation applied to the caudate nucleus directly because microstimulation activates neurons around the tip of the electrode nonselectively.

Conclusion

By controlling the timing of microstimulation precisely, we have established that both poststimulus and prestimulus activities of caudate neurons are sufficient to control saccade initiation. This complements our previous findings that the activity of caudate neurons is correlated with saccade RTs on a trial-by-trial basis (Watanabe & Munoz, 2009, 2010b). Our results support the hypothesis that the BG contribute to flexible saccadic behavior by controlling both poststimulus and prestimulus activities of neurons in structures tightly related to saccade initiation, such as the SC and the FEF. In future research, it will be important to test these hypotheses, for instance, by combining caudate microstimulation and the blockage of signal transmission through the indirect pathway with drug microinjections (e.g., GABA antagonists in GPe and glutamate antagonists in STN) to understand how caudate signals are processed through the cortex–BG circuits to influence saccade RTs.

Acknowledgments

The authors thank A. Lablans and R. Cranham for animal care, F. Paquin, S. Hickman, R. Pengelly, and M. Lewis for technical assistance, and members of the Munoz laboratory for comments on this manuscript. This work was supported by the Canadian Institutes of Health Research (MOP-77734). DPM was supported by the Canadian Research Chair Program.

Reprint requests should be sent to Douglas P. Munoz, Centre for Neuroscience Studies, Queen's University, Room 234, Botterell Hall, 18 Stuart Street, Kingston, Ontario, Canada K7L3N6, or via e-mail: doug_munoz@biomed.queensu.ca.

REFERENCES

Alexander, G. E., DeLong, M. R., & Strick, P. L. (1986). Parallel organization of functionally segregated circuits linking basal ganglia and cortex. *Annual Review of Neuroscience, 9,* 357–381.

Basso, M. A., & Liu, P. (2007). Context-dependent effects of substantia nigra stimulation on eye movements. *Journal of Neurophysiology, 97,* 4129–4142.

Basso, M. A., & Wurtz, R. H. (2002). Neuronal activity in substantia nigra pars reticulata during target selection. *Journal of Neuroscience, 22,* 1883–1894.

Bell, A. H., Everling, S., & Munoz, D. P. (2000). Influence of stimulus eccentricity and direction on characteristics of pro- and antisaccades in non-human primates. *Journal of Neurophysiology, 84,* 2595–2604.

Boucher, L., Palmeri, T. J., Logan, G. D., & Schall, J. D. (2007). Inhibitory control in mind and brain: An interactive race model of countermanding saccades. *Psychological Review, 114,* 376–397.

Burman, D. D., & Bruce, C. J. (1997). Suppression of task-related saccades by electrical stimulation in the primate's frontal eye field. *Journal of Neurophysiology, 77,* 2252–2267.

Carpenter, R. H., & Williams, M. L. (1995). Neural computation of log likelihood in control of saccadic eye movements. *Nature, 377,* 59–62.

Carpenter, R. H. S. (1981). Oculomotor procrastination. In D. F. Fischer & R. A. Monty (Eds.), *Eye movements: Cognition and visual perception* (pp. 237–246). Hillsdale, NJ: Erlbaum.

Cebrian, C., Parent, A., & Prensa, L. (2005). Patterns of axonal branching of neurons of the substantia nigra pars reticulata and pars lateralis in the rat. *Journal of Comparative Neurology, 492,* 349–369.

Crist, C. F., Yamasaki, D. S., Komatsu, H., & Wurtz, R. H. (1988). A grid system and a microsyringe for single cell recording. *Journal of Neuroscience Methods, 26,* 117–122.

Dafoe, J. M., Armstrong, I. T., & Munoz, D. P. (2007). The influence of stimulus direction and eccentricity on pro- and anti-saccades in humans. *Experimental Brain Research, 179,* 563–570.

DeAngelis, G. C., & Uka, T. (2003). Coding of horizontal disparity and velocity by MT neurons in the alert macaque. *Journal of Neurophysiology, 89,* 1094–1111.

Dorris, M. C., Olivier, E., & Munoz, D. P. (2007). Competitive integration of visual and preparatory signals in the superior colliculus during saccadic programming. *Journal of Neuroscience, 27,* 5053–5062.

Dorris, M. C., Pare, M., & Munoz, D. P. (1997). Neuronal activity in monkey superior colliculus related to the initiation of saccadic eye movements. *Journal of Neuroscience, 17,* 8566–8579.

Everling, S., & Fischer, B. (1998). The antisaccade: A review of basic research and clinical studies. *Neuropsychologia, 36,* 885–899.

Everling, S., & Munoz, D. P. (2000). Neuronal correlates for preparatory set associated with pro-saccades and anti-saccades in the primate frontal eye field. *Journal of Neuroscience, 20,* 387–400.

Fischer, B., & Weber, H. (1992). Characteristics of "anti" saccades in man. *Experimental Brain Research, 89,* 415–424.

Fischer, B., & Weber, H. (1993). Express saccades and visual attention. *Behavioral and Brain Sciences, 16,* 553–610.
Ford, K. A., & Everling, S. (2009). Neural activity in primate caudate nucleus associated with pro- and antisaccades. *Journal of Neurophysiology, 102,* 2334–2341.
Francois, C., Yelnik, J., & Percheron, G. (1996). A stereotaxic atlas of the basal ganglia in macaques. *Brain Research Bulletin, 41,* 151–158.
Fuchs, A. F., & Robinson, D. A. (1966). A method for measuring horizontal and vertical eye movement chronically in the monkey. *Journal of Applied Physiology, 21,* 1068–1070.
Hallett, P. E. (1978). Primary and secondary saccades to goals defined by instructions. *Vision Research, 18,* 1279–1296.
Handel, A., & Glimcher, P. W. (1999). Quantitative analysis of substantia nigra pars reticulata activity during a visually guided saccade task. *Journal of Neurophysiology, 82,* 3458–3475.
Hanes, D. P., & Schall, J. D. (1996). Neural control of voluntary movement initiation. *Science, 274,* 427–430.
Hikosaka, O., Sakamoto, M., & Miyashita, N. (1993). Effects of caudate nucleus stimulation on substantia nigra cell activity in monkey. *Experimental Brain Research, 95,* 457–472.
Hikosaka, O., Sakamoto, M., & Usui, S. (1989a). Functional properties of monkey caudate neurons: III. Activities related to expectation of target and reward. *Journal of Neurophysiology, 61,* 814–832.
Hikosaka, O., Sakamoto, M., & Usui, S. (1989b). Functional properties of monkey caudate neurons: I. Activities related to saccadic eye movements. *Journal of Neurophysiology, 61,* 780–798.
Hikosaka, O., Takikawa, Y., & Kawagoe, R. (2000). Role of the basal ganglia in the control of purposive saccadic eye movements. *Physiological Reviews, 80,* 953–978.
Hikosaka, O., & Wurtz, R. H. (1983a). Visual and oculomotor functions of monkey substantia nigra pars reticulata: III. memory-contingent visual and saccade responses. *Journal of Neurophysiology, 49,* 1268–1284.
Hikosaka, O., & Wurtz, R. H. (1983b). Visual and oculomotor functions of monkey substantia nigra pars reticulata: IV. Relation of substantia nigra to superior colliculus. *Journal of Neurophysiology, 49,* 1285–1301.
Huerta, M. F., & Kaas, J. H. (1990). Supplementary eye field as defined by intracortical microstimulation: Connections in macaques. *Journal of Comparative Neurology, 293,* 299–330.
Isoda, M. (2005). Context-dependent stimulation effects on saccade initiation in the presupplementary motor area of the monkey. *Journal of Neurophysiology, 93,* 3016–3022.
Itoh, H., Nakahara, H., Hikosaka, O., Kawagoe, R., Takikawa, Y., & Aihara, K. (2003). Correlation of primate caudate neural activity and saccade parameters in reward-oriented behavior. *Journal of Neurophysiology, 89,* 1774–1783.
Izawa, Y., Suzuki, H., & Shinoda, Y. (2004a). Suppression of visually and memory-guided saccades induced by electrical stimulation of the monkey frontal eye field: II. Suppression of bilateral saccades. *Journal of Neurophysiology, 92,* 2261–2273.
Izawa, Y., Suzuki, H., & Shinoda, Y. (2004b). Suppression of visually and memory-guided saccades induced by electrical stimulation of the monkey frontal eye field: I. Suppression of ipsilateral saccades. *Journal of Neurophysiology, 92,* 2248–2260.
Jiang, H., Stein, B. E., & McHaffie, J. G. (2003). Opposing basal ganglia processes shape midbrain visuomotor activity bilaterally. *Nature, 423,* 982–986.
Johnston, K., & Everling, S. (2006). Monkey dorsolateral prefrontal cortex sends task-selective signals directly to the superior colliculus. *Journal of Neuroscience, 26,* 12471–12478.
Judge, S. J., Richmond, B. J., & Chu, F. C. (1980). Implantation of magnetic search coils for measurement of eye position: An improved method. *Vision Research, 20,* 535–538.
Kawagoe, R., Takikawa, Y., & Hikosaka, O. (1998). Expectation of reward modulates cognitive signals in the basal ganglia. *Nature Neuroscience, 1,* 411–416.
Kitama, T., Ohno, T., Tanaka, M., Tsubokawa, H., & Yoshida, K. (1991). Stimulation of the caudate nucleus induces contraversive saccadic eye movements as well as head turning in the cat. *Neuroscience Research, 12,* 287–292.
Luppino, G., Matelli, M., Camarda, R. M., Gallese, V., & Rizzolatti, G. (1991). Multiple representations of body movements in mesial area 6 and the adjacent cingulate cortex: An intracortical microstimulation study in the macaque monkey. *Journal of Comparative Neurology, 311,* 463–482.
Marino, R. A., Rodgers, C. K., Levy, R., & Munoz, D. P. (2008). Spatial relationships of visuomotor transformations in the superior colliculus map. *Journal of Neurophysiology, 100,* 2564–2576.
Mikula, S., Trotts, I., Stone, J. M., & Jones, E. G. (2007). Internet-enabled high-resolution brain mapping and virtual microscopy. *Neuroimage, 35,* 9–15.
Miyashita, N., & Hikosaka, O. (1996). Minimal synaptic delay in the saccadic output pathway of the superior colliculus studied in awake monkey. *Experimental Brain Research, 112,* 187–196.
Munoz, D. P., & Everling, S. (2004). Look away: The anti-saccade task and the voluntary control of eye movement. *Nature Reviews Neuroscience, 5,* 218–228.
Munoz, D. P., & Wurtz, R. H. (1993). Fixation cells in monkey superior colliculus: II. Reversible activation and deactivation. *Journal of Neurophysiology, 70,* 576–589.
Nachev, P., Kennard, C., & Husain, M. (2008). Functional role of the supplementary and pre-supplementary motor areas. *Nature Reviews Neuroscience, 9,* 856–869.
Nakahara, H., Nakamura, K., & Hikosaka, O. (2006). Extended LATER model can account for trial-by-trial variability of both pre- and post-processes. *Neural Networks, 19,* 1027–1046.
Nakamura, K., & Hikosaka, O. (2006). Facilitation of saccadic eye movements by postsaccadic electrical stimulation in the primate caudate. *Journal of Neuroscience, 26,* 12885–12895.
Nambu, A., Tokuno, H., Hamada, I., Kita, H., Imanishi, M., Akazawa, T., et al. (2000). Excitatory cortical inputs to pallidal neurons via the subthalamic nucleus in the monkey. *Journal of Neurophysiology, 84,* 289–300.
Pare, M., & Hanes, D. P. (2003). Controlled movement processing: Superior colliculus activity associated with countermanded saccades. *Journal of Neuroscience, 23,* 6480–6489.
Person, A. L., & Perkel, D. J. (2005). Unitary IPSPs drive precise thalamic spiking in a circuit required for learning. *Neuron, 46,* 129–140.
Phillips, J. M., Johnston, K., & Everling, S. (2011). Effects of anterior cingulate microstimulation on pro- and antisaccades in nonhuman primates. *Journal of Cognitive Neuroscience, 23,* 481–490.
Ratcliff, R., & Tuerlinckx, F. (2002). Estimating parameters of the diffusion model: Approaches to dealing with contaminant reaction times and parameter variability. *Psychonomic Bulletin & Review, 9,* 438–481.

Reddi, B. A., Asrress, K. N., & Carpenter, R. H. (2003). Accuracy, information, and response time in a saccadic decision task. *Journal of Neurophysiology, 90,* 3538–3546.
Robinson, D. A. (1963). A method of measuring eye movement using a scleral search coil in a magnetic field. *IEEE Transactions on Biomedical Engineering, 10,* 137–145.
Sato, M., & Hikosaka, O. (2002). Role of primate substantia nigra pars reticulata in reward-oriented saccadic eye movement. *Journal of Neuroscience, 22,* 2363–2373.
Smith, P. L., & Ratcliff, R. (2004). Psychology and neurobiology of simple decisions. *Trends in Neurosciences, 27,* 161–168.
Stuphorn, V., & Schall, J. D. (2006). Executive control of countermanding saccades by the supplementary eye field. *Nature Neuroscience, 9,* 925–931.
Tachibana, Y., Kita, H., Chiken, S., Takada, M., & Nambu, A. (2008). Motor cortical control of internal pallidal activity through glutamatergic and GABAergic inputs in awake monkeys. *European Journal of Neuroscience, 27,* 238–253.
Takikawa, Y., Kawagoe, R., & Hikosaka, O. (2002). Reward-dependent spatial selectivity of anticipatory activity in monkey caudate neurons. *Journal of Neurophysiology, 87,* 508–515.
Trappenberg, T. P., Dorris, M. C., Munoz, D. P., & Klein, R. M. (2001). A model of saccade initiation based on the competitive integration of exogenous and endogenous signals in the superior colliculus. *Journal of Cognitive Neuroscience, 13,* 256–271.
Wagenmakers, E. J. (2007). A practical solution to the pervasive problems of *p* values. *Psychonomic Bulletin & Review, 14,* 779–804.
Watanabe, K., Lauwereyns, J., & Hikosaka, O. (2003). Neural correlates of rewarded and unrewarded eye movements in the primate caudate nucleus. *Journal of Neuroscience, 23,* 10052–10057.
Watanabe, M., & Munoz, D. P. (2009). Neural correlates of conflict resolution between automatic and volitional actions by basal ganglia. *European Journal of Neuroscience, 30,* 2165–2176.
Watanabe, M., & Munoz, D. P. (2010a). Saccade suppression by electrical microstimulation in monkey caudate nucleus. *Journal of Neuroscience, 30,* 2700–2709.
Watanabe, M., & Munoz, D. P. (2010b). Presetting basal ganglia for volitional actions. *Journal of Neuroscience*, *30,* 10144–10157.
Wegener, S. P., Johnston, K., & Everling, S. (2008). Microstimulation of monkey dorsolateral prefrontal cortex impairs antisaccade performance. *Experimental Brain Research, 190,* 463–473.
Yang, S. N., Heinen, S. J., & Missal, M. (2008). The effects of microstimulation of the dorsomedial frontal cortex on saccade latency. *Journal of Neurophysiology, 99,* 1857–1870.
Yoshida, A., & Tanaka, M. (2009). Enhanced modulation of neuronal activity during antisaccades in the primate globus pallidus. *Cerebral Cortex, 19,* 206–217.